Applied Thermal Engineering 239 (2024) 122129

Contents lists available at ScienceDirect

Applied Thermal Engineering

journal homepage: www.elsevier.com/locate/apthermeng

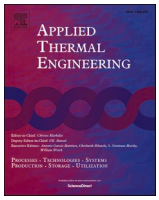

Research Paper

Energy and cost analysis for a crop production in a vertical farm

A. Arcasi [a], A.W. Mauro [a,*], G. Napoli [b], F. Tariello [c], G.P. Vanoli [b]

[a] Università degli Studi di Napoli Federico II, Department of Industrial Engineering, Piazzale Tecchio 80, 80125 Napoli, Italy
[b] Università degli Studi del Molise, Department of Medicine and Health Sciences, Via Francesco de Sacntis 1, 86100 Campobasso, Italy
[c] Università degli Studi del Molise, Department of Agricultural, Environment and Food Sciences, Via Francesco de Sacntis 1, 86100 Campobasso, Italy

ARTICLE INFO

Keywords:
Vertical farm
Energy specific cost
Energy consumption
Parametric assessment
Dynamic simulation
Lettuce production

ABSTRACT

Nowadays, the agricultural sector is undermined by arable land and water availability. Vertical farms represent an interesting solution offering the possibility to overcome these issues also reducing pesticides use. However, their high energy demands make it crucial to develop an effective methodology to attribute the specific energy cost to the kilogram of each product harvested. A multi-level model considering the elements that intervene in the energy balance characterizing the cultivation phase in vertical farms is introduced below. A parametric analysis is carried out with it, considering different cities and multiple scenarios in terms of lighting efficiency and intensity, leaf surface temperature, electricity and natural gas cost. The results unveil a strong dependence of the total energy consumption and the specific cost of the product on external conditions, such as the climate, the efficiency of the electric national system and the energy cost. Notably, in Riyadh, the energy consumption (10.1 $GWh \bullet year^{-1}$) is up to 86% higher than in Stockholm and 38% higher than in Naples. By means of the internal conditions' optimization, the specific cost for energy of the lettuce production in the vertical farm growth chamber, is 0.85 $€ \bullet kg^{-1}$ in Stockholm, 1.35 $€ \bullet kg^{-1}$ in Naples and 1.75 $€ \bullet kg^{-1}$ in Riyadh.

1. Introduction

In the last decades, the water-energy-food nexus has been strained by numerous and significant challenges. The global population constant growth, rapid urbanization, pest use, climate change, resource degradation and scarcity have all placed immense pressure on the agricultural sector, which is the largest water consumer [1], with a forecasted increase by about 55 % by 2050 [2]. Furthermore, in 2021 it contributed for 3 % of energy consumption [3] in Europe. Additionally, energy demand is expected to increase worldwide, reaching about 22 Gtoe in 2050 [4].

Moreover, the reduction in cropland per capita [5], the global population growth [6,7] and the rapid urbanization [6], will exacerbate the scarcity of arable land and water resources. Furthermore, the extensive use of pesticides and inorganic fertilizers also has detrimental effects on the quality of agricultural products [8].

In addition, at present, approximately 795 million individuals worldwide suffer from malnutrition, and over 1.4 billion people lack access to electricity, and the resulting energy shortage stands as a significant barrier to producing sufficient food to meet global demand. All the aforementioned issues have compelled the United Nations to establish various goals to be achieved by 2030 and 2050 [9], such as eradicating hunger, poverty, and malnutrition worldwide, while ensuring sustainable and healthy food production. To achieve these aims it is fundamental to enhance the productivity of traditional farming method. However, since they rely on external climate conditions, huge water and land usage, it becomes necessary to develop alternative and low-environmental impact technologies for the agricultural sector. One of the most promising and potentially sustainable approaches in this context is indoor farming, specifically within completely closed and controlled environments known as plant factories or vertical farms (*VF*s). Vertical farms consist of well-insulated structures which create optimal conditions for plant growth, regulating temperature and relative humidity. Crops are arranged vertically on multiple layers, and the system incorporates lighting devices such as *LED* systems or fluorescent lamps to replace natural sunlight. Air conditioning systems are employed for cooling and dehumidification, while CO_2 units monitor and maintain optimal CO_2 levels. Additionally, *VF*s are equipped with nutrient solution and water supply systems [10,11]. Thanks to their advantages, such as water and CO_2 savings and healthy food production, *VF*s are becoming more and more widespread especially in hostile climate regions where few lighting hours and/or water scarcity occur [12] and they can be installed in urban context by reducing cost and

* Corresponding author.
E-mail address: wmauro@unina.it (A.W. Mauro).

https://doi.org/10.1016/j.applthermaleng.2023.122129
Received 2 August 2023; Received in revised form 20 October 2023; Accepted 27 November 2023
Available online 1 December 2023

Nomenclature

A	surface area $[m^2]$
AHU	air handling unit
c	specific heat
CAC	cultivation area cover [−]
cos	cosine [−]
c_{el}	specific cost of electricity
c_{gas}	specific cost of natural gas [€ • Sm^{-3}]
e	specific energy consumption [kWh • kg^{-1}]
E	primary energy consumption,[kWh]
EER	energy efficiency ratio [−]
F	yield proportionality factor [−]
G	solar radiation [W • m^{-2}]
GHG	greenhouse gas emission
h	convective heat transfer coefficient [W • m^{-2} • K^{-1}]
H	low heating value [kWh • m^{-3}]
HFO	hydro-fluoro-olefin
$HVAC$	heating, ventilation and air conditioning
i	specific enthalpy [kJ • kg^{-1}]
$\dot{I}_{net,canopy}$	thermal power intercepted by the plants [kW]
k	thermal conductivity [kW • m^{-1} • K^{-1}]
l	mean leaf diameter [m]
LAI	leaf area index [−]
LCA	life cycle assessment
LED	LED system
m	mass [kg]
$\dot{m}$	mass flow rate [$kg \bullet s^{-1}$]
M	number of the walls [−]
n	number [−]
N	number of elementary geometries [−]
P	pressure [kPa]
$\dot{P}$	electrical power [kW]
$PPFD$	photosynthetic photon flux density [$\mu mol \bullet m^{-2} \bullet s^{-1}$]
$\dot{q}$	heat flux [$kW \bullet m^{-2}$]
$\dot{Q}$	thermal power [kW]
r	resistance [$s \bullet m^{-1}$]
R	reflection coefficient [-]
SCE	specific cost for energy [€ • kg^{-1}]
$SEER$	seasonal energy efficiency ratio [−]
SHR	sensible to total heat ratio [−]
T	temperature [°C]
TCE	total cost of energy [€ • $year^{-1}$]
u	velocity [m • s^{-1}]
V	volume [m^3]
$\dot{V}$	volumetric flow rate [$m^3 \bullet h^{-1}$]
VCD	vapor concentration deficit [$kg \bullet m^{-3}$]
VF	vertical farm
x	wall thickness [m]
Y	production yield [$kg \bullet m^{-2}$]
$\dot{W}$	mechanical power [kW]

Greek symbols

α	absorption coefficient [−]
γ	angle of incidence of the solar radiation [rad]
δ	differential variation [−]
Δ	variation [−]
η	efficiency [−]
$\eta_{led,PAR}$	conversion factor $[\mu mol \bullet J^{-1}]$
ϑ	time [s]
ρ	density [$kg \bullet m^{-3}$]
Φ	relative humidity [%]
ω	specific humidity [$g_{vap} \bullet kg_{air}^{-1}$]

Subscripts and superscripts

$actual$	actual
air	related to air
Bo	boiler
$cell$	cell
Ch	chiller
$comp$	compressor
$cycle$	cycle
el	electric
ev	evaporator
$evap$	evaporated
ext	external
fan	fans
gas	natural gas
$grow$	grow
GC	growth chamber
i	i-th
in	inlet
int	internal
is	isoentropic
j	j-th
lat	latent
$leaf$	crop's leaf
LED	*LED* system
LED,PAR	photosynthetic active radiation of the *LED* system
$lettuce$	Related to lettuce
max	maximum
Mix	mixing
N	number of elements of the wall
opt	optimum
out	outlet
p	product
$plant$	related to plant
$PPFD$	photosynthetic photon flux density
$primary$	primary
ref	reference value
$refr$	refrigerant
$return$	return
s	stomatal
$sens$	sensible
$target$	target value
$temp$	temperature
tot	total
vap	vapor
w	water
$wall$	wall
∞	inhibited

emissions related to the transport of products to the final users [13,14]. In literature, several studies argue the possibility to employ vertical farm systems by analyzing their techno-economic feasibility from different points of view. Kozai [10] conducted a comparative analysis between greenhouse and vertical farm systems, considering water usage, CO_2 emissions, electricity consumption, and inorganic fertilizer usage. This study found that vertical farms exhibit lower water and CO_2 usage compared to greenhouses, with reduction by, respectively, 50 and 1.8 times.

However, *VF*s consume 2.5 times more energy due to their lighting

systems compared to greenhouses. Similar results were observed in Harbrick et al.'s study [15] which simulated and compared *VF*s and greenhouses founding that *VF*s reach up to 11 and 13 times higher energy consumption and CO_2 emissions. Graamans et al. [12] compared greenhouse and *VF* systems for lettuce production in three different climate zones. Vertical farms exhibited higher and more stable productivity throughout the year compared to greenhouses, with a twofold increase, 95 % lower water usage but, conversely, higher electricity consumption. Park et al. [16] compared *VF* and open field methods, finding that the first allow to achieve higher crop production with lower levels of fungicides and pesticides. Finally, Avgousaki et al. [17] conducted a comparison between vertical farms and greenhouses for basil production, founding that *VF*s offer significantly higher resource savings compared to greenhouse systems.

The energy consumption aspect remains a significant challenge for indoor farming methods. Consequently, various studies have explored possibilities for reducing energy consumption from different perspectives. Molin et al. [18], observed that in *VF*s the dry matter harvested per production area is 17.5 % higher than in open field. Moreover, they found that lighting system is responsible up to 45 % of the total greenhouse gas emissions. Martin et al. [19], through the *LCA* (life cycle assessment) method quantified the cradle-to-grave environmental impact for 1 kg of lettuce produced in a vertical farm in Sweden, corresponding to 0.98 kg $CO_{2\text{-eq}} \bullet kg^{-1}$ of *GHG* emissions.

Graamans et al. [20] conducted a study by considering three different climate zones and the crop transpiration model developed in [21] was coupled with the building energy simulation software EnergyPlus. They found that with opaque façades and by optimizing the timing of the lighting and darkness period, a significant energy consumption reduction can be achieved.

Avgoustaki [22] developed an optimization algorithm in MATLAB to achieve consumption reduction, resulting in energy savings ranging from 16 % to 26 %. Yalcin et al. [23] explored a solar illumination design using fluorescent coatings to enhance crop production, estimating an increase by up to 35 %.

Additionally, Weidner et al. [24] validated an energy consumption optimization model for vertical farms, greenhouses, and open fields in Stockholm, extending its application to different climate zones, revealing that *VF* systems are more energy-intensive compared to greenhouses in all analyzed locations.

To the best of authors' knowledge, there is a growing scientific interest in analyzing alternative/innovative cultivation systems, like vertical farms, today. These studies focus on specific aspects affecting the production in *VF*. Some studies take into account the lighting system efficiency [25], some others the optimal canopy temperature for plant growth [26,27], some of the other the indoor and outdoor climatic conditions to [24]. Hereinafter, instead, the authors introduce a multi-level model of the entire vegetable production system in *VF*, that allows to determine the primary energy demands and the energy costs linked to the product unit. Particularly, the multi-level models encompass the plant sub-model, through which the energy balance on the leaf surface is evaluated in steady state conditions, then the dynamic energy balance on the *VF* structure sub-model, taking into account the plants contributions (sensible and latent), the unexploited light power in the process of photosynthesis, all the heat transfers through the building envelope and the contribution of the air-conditioning system, evaluated in its sensible and latent shares necessary to continuously hold the target values of temperature and relative humidity.

Additionally, an economic model is presented to quantify the energy required to produce one kilogram of lettuce in the vertical farm under consideration, thereby determining its associated cost. In particular, two indexes are introduced in the present work, namely the primary energy consumption associated to the growth phase ($E_{primary}$), and the specific cost for energy (*SCE*), which allow to allocate the cost of energy on the kilogram of each harvested product.

This approach is intended to pave the way for a general procedure to evaluate the specific energy cost of any kind of product unit, highlighting the different contributions that determine the total energy cost of a product and so identifying the most energy intensive ones, those to be optimized.

The case study encompasses the layout of the vertical farm in three different cities, namely Naples, Riyadh and Stockholm, representative of three climatic condition, according to Köppen–Geiger climate classification: Csa - Hot-summer Mediterranean climate, BWh - Hot desert climate and Dbf - Warm summer humid continental climate, respectively. Furthermore, a sensitivity analysis is conducted by varying the optimal plant temperature during the growth phase, the photosynthetic photon flux density, and the efficiency of the lighting system, to quantify the influence of each parameter on total and specific energy consumption and costs. Finally, the results concerning the energetic and economic aspects are described and discussed.

2. Vertical farm growth chamber model

Vertical farm (*VF*) systems consist of multiple areas serving different purposes. However, this work specifically focuses on crop growth chamber. After that the plant's early stages of development take place in the germination chamber, the crops are transferred to the main growth room where most of the growth occurs. Therefore, this work assesses the energy consumption of this area of the *VF*: Fig. 1 provides a schematic representation of *VF* growth chamber, illustrating the various energy loads occurring in a control volume comprising the aforesaid chamber, with the frontier on internal walls. Specifically, $\dot{P}_{led}$ is the electrical power absorbed by the *LED*, $\dot{Q}_{wall,tot}$ is the heat transfer through the building envelope, and then, with a focus on the energy balance on the crop, which is in steady state condition, $\dot{I}_{net,canopy}$ is the active radiation adsorbed by the plant and participating to the photosynthesis process, $\dot{Q}_{lat,plant}$ and $\dot{Q}_{sens,plant}$ are latent and sensible heat associated with plants metabolism, respectively. All the thermal load, both latent and sensible, are counterbalanced by an *HVAC* system, consisting of an Air Handling Unit (*AHU*) operating mainly with recirculating air (only 5 % fresh air), that is suitably conditioned through heating and cooling coils equipping the *AHU* and fed by a natural gas boiler and an electric chiller, respectively.

2.1. Plants transpiration and energy balance

The crop is the principal item in the growth chamber, affecting tremendously the overall energy balance, absorbing radiation, exchanging heat with the environment and finally transpiring. Particularly, it absorbs a certain amount of radiation which is then released as sensible and latent heat in steady state conditions. Thus, the thermal power intercepted by the crops is evaluated with Eq (1):

$$\dot{I}_{net,canopy} = \dot{P}_{led} \bullet \eta_{led} \bullet CAC \bullet (1 - R) \tag{1}$$

Where η_{led}, is the electric efficiency of the *LED*s, *CAC* is the cultivation area cover factor (being the ratio between plant leaf surface and plant bad surface), that is 0.95, and *R* is the reflection coefficient, assumed to be 0.05. The radiation that reaches the plants is not entirely employed to trigger the photosynthesis process, thus the photosynthetic photon flux density (*PPFD*), which is the amount active in the photosynthesis, is evaluated with Eq. (2):

$$PPFD = \dot{I}_{net,canopy} \bullet \eta_{led,PAR} \tag{2}$$

Where $\eta_{led,PAR}$ is a conversion factor, depending on the technology employed for lighting, indicating the contributing *J* of the radiation converted in μmol employed for plant growth.

The latent thermal power, caused by the evapotranspiration process of the canopy, is evaluated with the model developed by Graamans et al. [21]:

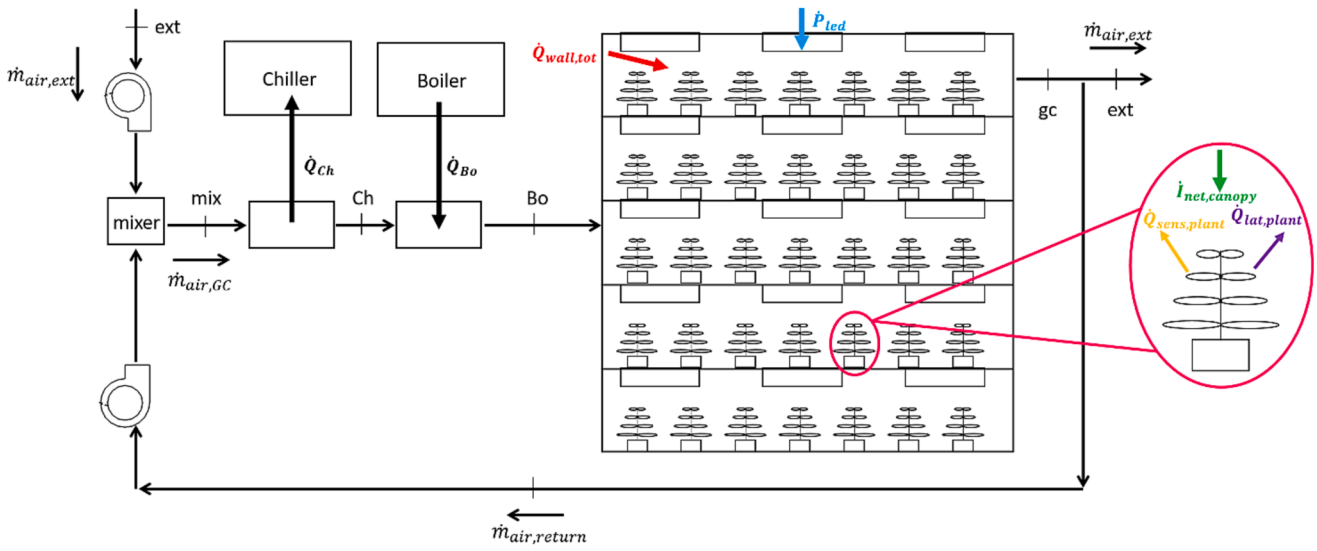

Fig. 1. Schematization of the growth chamber and systems serving the plant, highlighting the energy flows over a control volume with the frontier on the growth chamber internal walls.

$$\dot{Q}_{lat,plant} = \dot{q}_{lat,plant} \bullet A_{grow} \tag{3}$$

In Eq. (3) $\dot{q}_{lat,plant}$ is the latent heat flux caused by the crops evapotranspiration, while A_{grow} is the total cultivation area. $\dot{q}_{lat,plant}$ and the water mass flow rate transpired are evaluated with Eqs. (4–5):

$$\dot{q}_{lat,plant} = LAI \bullet \Delta i_w \bullet \frac{VCD}{r_s + r_{air}} \tag{4}$$

$$\dot{m}_{w,evap} = \frac{\dot{Q}_{lat,plant}}{\Delta i_w} \tag{5}$$

In the previous equations, *LAI* (leaf area index) is the green leaf area per unit ground surface area, assumed to be constant in this work being an averaged value of the different growth stage. Δi_w is the latent heat of vaporization on the leaf surface, and it is the water latent heat at leaf surface temperature. Moreover, *VCD* is the vapor concentration deficit between canopy and air. Finally, r_s and r_{air} are, respectively, the leaf surface and aerodynamic resistance to vapor transfer. These two terms are evaluated with Eqs. (6–7):

$$r_{air} = 350 \bullet \left(\frac{l}{u_\infty}\right)^{0.5} \bullet LAI^{-1} \tag{6}$$

$$r_s = 60 \bullet \frac{1500 + PPFD}{200 + PPFD} \tag{7}$$

Where l is the mean leaf diameter, considered to be constant for the same assumption made for the *LAI*, and u_∞ is the uninhibited air velocity.

The sensible thermal power exchanged with the surrounding environment is evaluated by closing the energy balance on the plant, according to Eq. (8):

$$\dot{Q}_{sens,plant} = \dot{I}_{net,canopy} - \dot{Q}_{lat,plant} \tag{8}$$

Consequently, the sensible heat flux is evaluated with Eq. (9):

$$\dot{q}_{sens,plant} = \frac{\dot{Q}_{sens,plant}}{A_{grow}} \tag{9}$$

Since the sensible heat transfer is dominated by a temperature difference between the leaf surface and the surrounding environment, knowing the leaf surface temperature, it is possible to calculate the growth cell's temperature, which is the proper value to ensure the optimal temperature on the leaf in order to maximize the yield:

$$T_{cell} = T_{leaf} - \frac{\dot{q}_{sens,plant} \bullet r_{air}}{\rho_{air} \bullet c_{p,air} \bullet LAI} \tag{10}$$

ρ_{air} and $c_{p,air}$ are, respectively, the air density and heat capacity.

2.2. Heat transfer with the environment

Solved the crop energy model and evaluated the cell temperature necessary to guarantee the desired leaf temperature, the heat exchange through the building envelope is calculated. The total heat transfer is the sum of the heat exchange across each *j-th* wall constituting the building envelope (neglecting the terms related to the ground heat exchange), as reported in Eq. (11).

$$\dot{Q}_{wall,tot} = \sum_{j=1}^{M} \dot{Q}_{wall,j} \tag{11}$$

The heat power for the generic *j-th* wall, at each time step is given by Eq. (12):

$$\dot{Q}_{wall,i,j} = h_{int} \bullet A_j \bullet \left(T_{1,i} - T_{cell,i}\right) \tag{12}$$

Where, h_{int} is the internal convective heat transfer coefficient, which value ($7.7\ W \bullet m^{-2} \bullet K^{-1}$) is taken from [28], A_j is the transversal area of the generic *j-th* wall, changing according to the façade of the building envelope considered. Then, $T_{1,i}$ is the temperature of the inner surface of the *j-th* wall and $T_{cell,i}$ is the inner temperature in the cell at the *i-th* time step.

Thus, to evaluate the heat transfer through the building envelope, the wall temperature profile has to be solved. For this reason, a one-dimensional transient heat transfer equation is applied at each time step dividing the wall into *N* elementary geometries, having the same thickness, as shown in Fig. 2, distinguishing between the $\dot{Q}_{wall,j}$ and $\dot{Q}_{ext,j}$, in order to take into account the internal convective heat transfer, the conductive one through the wall, the external heat exchange by natural convection with the environment, the solar radiation on the walls and the thermal inertia of the building envelope. The one-dimensional hypothesis is valid since the wall thickness is significantly smaller than its surface.

The discretized form of energy balance on each *n-th* element constituting the wall allows to evaluate the temperature variation on

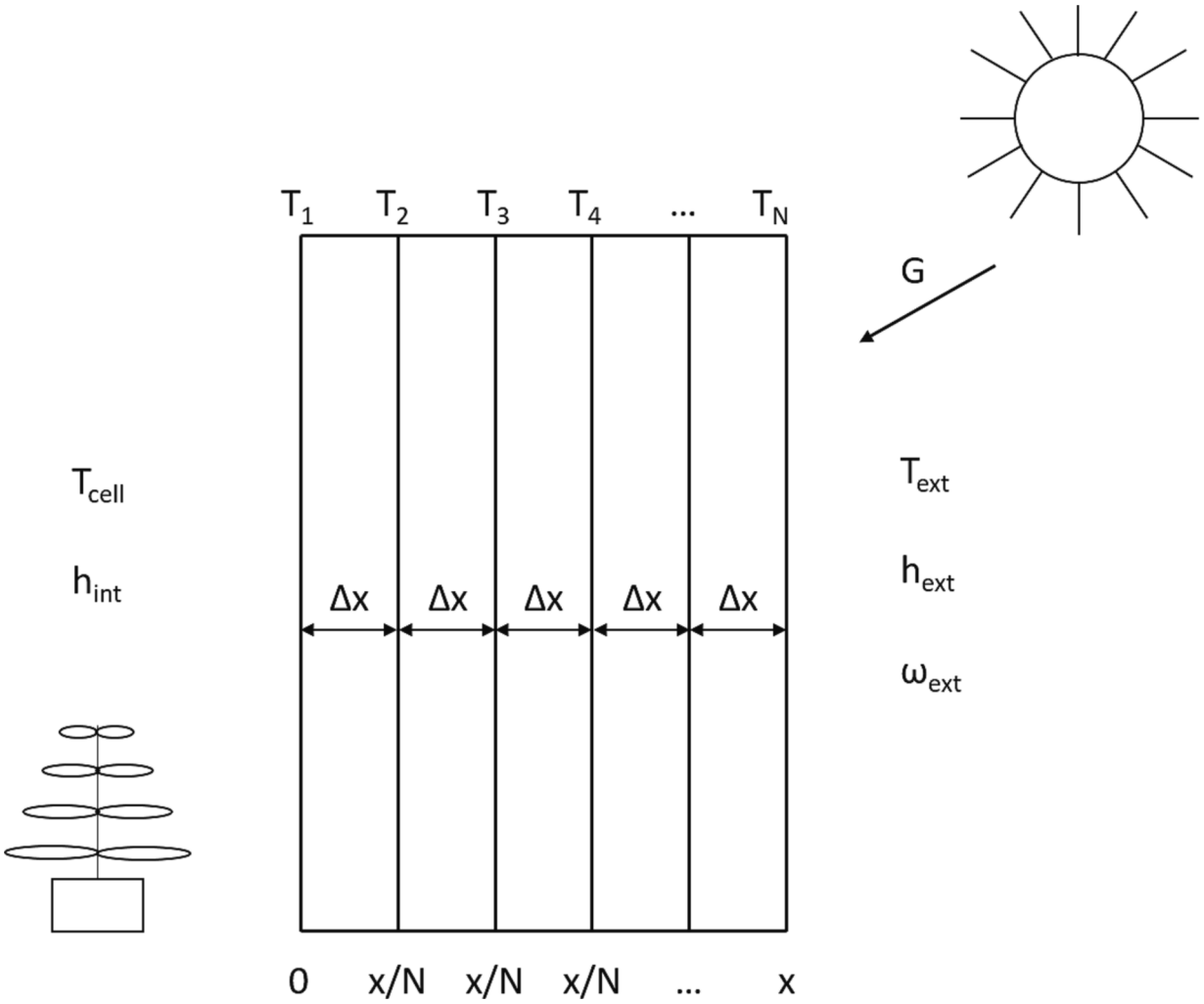

Fig. 2. Schematization of the generic wall of the building envelope.

each layer at the time step *i-th* (integration step of 60 s) treated as a node, employing the forward Eulerian method, allowing to calculate the temperature derivative (δT) with respect to the time derivative ($\delta\vartheta$), as reported in the following equations:

$$\frac{\delta T_{1,i}}{\delta\vartheta} = \frac{k_{wall} \bullet A_j \bullet \frac{\left(T_{2,i} - T_{1,i}\right)}{\Delta x} - h_{int} \bullet A_{j,i} \bullet \left(T_{1,i} - T_{cell,i}\right)}{\rho_{wall} \bullet V_1 \bullet c_{wall}} \tag{13}$$

$$\frac{\delta T_{n,i}}{\delta\vartheta} = \frac{k_{wall} \bullet A_j \bullet \left(T_{n+1,i} - T_{n,i}\right) - k_{wall,i} \bullet A_j \bullet \left(T_{n,i} - T_{n-1,i}\right)}{\Delta x \bullet \rho_{wall} \bullet V_n \bullet c_{wall}} \tag{14}$$

$$\frac{\delta T_{N,i}}{\delta\vartheta} = \frac{\left(h_{ext,i} \bullet A_j \bullet \left(T_{ext,i} - T_{N,i}\right) - k_{wall} \bullet A_j \bullet \frac{T_{N,i} - T_{N-1,i}}{\Delta x}\right) + G_i \bullet A_j \bullet \alpha \bullet cos(\gamma)}{\rho_{wall} \bullet V_N \bullet c_{wall}} \tag{15}$$

For the inner wall, as described in Eq. (13), there are both conductive and convective heat transfer, respectively with the adjacent layer of the wall and the air in the cell. k_{wall}, c_{wall} and ρ_{wall} are the thermal conductivity, the specific heat and the density of the insulating material employed in the wall, which is a polyurethane foam, having a total thickness equal to x, thus the thickness of each layer, Δx, is equal to $x \bullet N^{-1} \bullet V_n$ is the volume of each layer. For the intermediate layers, from the 2nd to *N-1* one, only conductive heat exchange with the two adjacent layers occurs, according to Eq. (14). For the external layer, as shown in Eq. (15), there is the convective heat exchange with the adjacent layer, convective one with the external environment and irradiance due to the solar radiation. In this equation, h_{ext} is the external heat transfer coefficients evaluated with calibrated correlation from the scientific literature as a function of the external wind velocity [29]. T_{ext} is the external temperature, G is the solar radiation, α is the absorption coefficient, and γ is the incidence angle of the solar radiation.

The analysis was carried out by considering the hourly temperature, irradiation, wind velocity and relative humidity profile during the whole year for each climate considered.

2.3. Air conditioning system model

The adequate conditions for the optimal crop growth are achieved by means an air conditioning system, balancing the sensible and latent loads, and ensuring the desired temperature and humidity in the room. Particularly, the *HVAC* system is made up by an Air Handling Unit consisting of a mixing section, where recirculated air is mixed with the external one, a cooling and dehumidification coil fed with cold water supplied by an electric chiller, a heating coil fed by a gas boiler.

An example of the thermodynamic processes which the air undergoes in the *HVAC* system is shown in Fig. 3.

Particularly, the exhaust air from the growth chamber, at condition *GC*, is firstly mixed with the external one, at *Ext* conditions, depending on external temperature and humidity, in order to guarantee a renewal, although minimal (5 %), reaching *Mix* conditions, then the air is cooled and dehumidified in the chiller, reaching condition *Ch* and then, enters

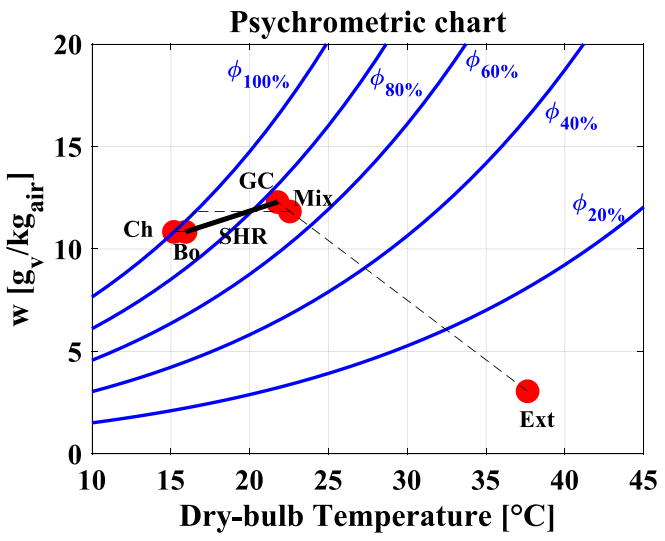

Fig. 3. Schematic of air transformation in the HVAC system on the psychometric chart.

the heating coil, where a gas boiler ensure the desired inlet conditions in the growth chamber, denominated *Bo*, that must rely on the Sensible Heat Ratio (*SHR*) line (all the points having the same sensible to total heat ratio), evaluated as:

$$SHR = \frac{\Delta i_{air}}{\Delta \omega} \tag{16}$$

Δi_{air} and $\Delta\omega$ are the air enthalpy and moisture differences between supply air and extract air from the cell (conditions *GC* and *Bo,* respectively), evaluated solving, simultaneously, the energy and vapor balance on moist air, Eqs. (17–18).

$$\dot{m}_{air,GC} = \frac{\dot{Q}_{wall,tot} + \dot{P}_{LED}}{i_{GC} - i_{Bo}} \tag{17}$$

$$\Delta\omega = \frac{\dot{m}_{w,evap}}{\dot{m}_{air,GC}} \tag{18}$$

Where $\dot{Q}_{wall,tot}$ is calculated with the model described in section 2.2, while the thermal load attributable to the lightning system corresponds exactly to its electrical power, $\dot{P}_{LED}$. i_{GC} and i_{Bo} are the moist air enthalpies at the exit and the inlet of the growth chamber. $\dot{m}_{w,evap}$ is the vapor flow rate related to the plants evapotranspiration, as evaluated in Eq. (5).

Regarding the chiller, it is a standard single-stage vapor compression cycle using R134a as refrigerant (whose transport and thermodynamic properties are calculated by using Refprop 9.1 [30] software), with the assumption that the system always counterbalances the total cooling and dehumidification load. A steady state lumped parameters approach has been followed.

The cooling capacity, $\dot{Q}_{Ch}$, is hourly evaluated with an energy balance on the air side:

$$\dot{Q}_{Ch} = \dot{m}_{air,GC} \bullet (i_{Ch} - i_{Mix}) \tag{19}$$

Knowing the required power from the chiller, with an energy balance on the evaporator, the refrigerant mass flow rate in the vapor compression cycle is calculated with Eq. (20):

$$\dot{m}_{refr} = \frac{\dot{Q}_{Ch}}{\Delta i_{refr} \bullet (1 - x_{in,ev})} \tag{20}$$

Where Δi_{ref} is the refrigerant latent heat at evaporator temperature and $x_{in,ev}$ is the vapor quality at evaporator inlet.

Then, the electric power required by the compressor is computed as follows:

$$\dot{W}_{comp} = \dot{m}_{refr} \bullet \frac{(i_{out,comp,is} - i_{in,comp})}{\eta_{comp}} \tag{21}$$

Where $i_{out,comp,is}$ is the enthalpy of the refrigerant at compressor outlet, considering an ideal isentropic compression, and $i_{in,comp}$ is the refrigerant enthalpy at compressor inlet, while η_{comp} is a function of compression ratio, using a polynomial correlation obtained from manufacturer data.

For each operating hour, the energy efficiency ratio, evaluated with Eq. (22) as required by the normative [31]:

$$EER = \frac{\dot{Q}_{Ch}}{\dot{W}_{comp}} \tag{22}$$

It is noteworthy that for each hour indoor and outdoor temperature variations are considered in Eq. (22), while the approach temperatures in the heat exchangers, the water temperature difference and the vapor quality at the condenser and evaporator outlet are unaffected by the boundary conditions and the load factor, with the fixed values reported in Table 1. This hypothesis is reliable due to the low approach temperature chosen, which would correspond to only low changes by varying the boundary conditions and thus, low EER changes in percentage.

Then, to prepare the heat transfer fluid for the heating coil, a boiler with an efficiency, η_{Bo}, of 0.9 is employed. The required power and the needed gas mass flow rate are given by the following equations:

$$\dot{Q}_{Bo} = \dot{m}_{GC} \bullet (i_{Bo} - i_{Ch}) \tag{23}$$

$$\dot{m}_{gas} = \frac{\dot{Q}_{Bo}}{H_{gas} \bullet \eta_{Bo}} \tag{24}$$

Where H_{gas} is the natural gas low heating value.

Finally, the circulation fans in the room have a power consumption given by the following:

$$\dot{W}_{fan} = \frac{\Delta P_{air} \bullet \dot{V}_{air}}{\eta_{fan}} \tag{25}$$

ΔP_{air} is the air's pressure drop through the heat exchangers, both the one in the chiller and the one in the re-heating coil, and across the ductworks, assuming an air velocity of 10 m • s^{-1}, $\dot{V}_{air}$ is the air volumetric flow rate, while η_{fan} is assumed to be 0.65.

2.4. Crop yield

The annual yield achievable is a function of different factors, both extensive and intensive. Particularly, as indicated in [24], with regard to lettuce, assuming a production cycle of 29 days, resulting in a number of producing cycle throughout the year, n_{cycle}, equal to 12, and a reference yield, Y_{ref}, of 6.25 $kg \bullet m^{-2}$, the annual yield is:

$$Y = F \bullet Y_{ref} \bullet A_{grow} \bullet n_{cycle} \tag{26}$$

In Eq. (26) *F* is a proportionality factor taking into account the dependency of productivity on lighting level and air temperature (while

Table 1
Main assumptions for vapor compression chiller simulation.

Parameter	Value
Refrigerant	R134a
Approach temperature in the evaporator [K]	3
Approach temperature in the condenser [K]	1
ΔT water [K]	3
Vapor quality at the evaporator outlet [-]	1
Vapor quality at the condenser outlet [-]	0

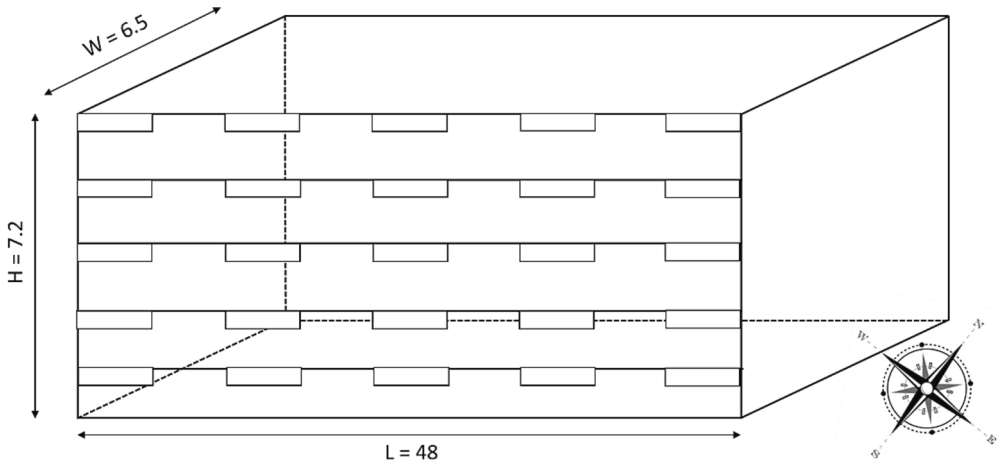

Fig. 4. Layout of the considered vertical farm with its dimensions and orientation.

the incidence of CO_2 level in the cell is here neglected since its value is assumed to be kept constant by a dedicated system). Particularly, F is made up by two terms:

$$F = F_{PPFD} \bullet F_{temp} \tag{27}$$

Where:

$$F_{PPFD} = \left(\frac{PPFD_{actual}}{PPFD_{target}} - 1\right) \bullet 0.74 + 1 \tag{28}$$

$$F_{temp} = \frac{T_{max} - T_{leaf}}{T_{max} - T_{opt}} * \left(\frac{T_{leaf}}{T_{opt}}\right)^{\frac{T_{opt}}{T_{max} - T_{opt}}} \tag{29}$$

In Eqs. (28–29) the F_{PPFD} and F_{temp} allows to take into account the yield modification occurring if *PPFD* and leaf temperature differ from the target. Particularly, $PPFD_{target}$, T_{max} and T_{opt}, are respectively the *PPFD* intensity scheduled for the cultivation, the maximum admissible temperature for the crop growth and the optimal one [24].

2.5. Economic model

With the models previously shown, it is possible to relate energy consumption to yield and to quantify the energy required in the growth chamber to produce a specific vegetable in a *VF*, and consequently the cost of the energy on the final product.

Particularly, the total primary energy consumption of the growth cell of the vertical farm is evaluated with Eq. (30):

$$E_{primary} = \sum_{i=1}^{T_{lettuce}} \left(\frac{\dot{Q}_{Ch}}{COP \bullet \eta_{el}} + \frac{\dot{P}_{led}}{\eta_{el}} + \frac{\dot{W}_{fan}}{\eta_{fan} \bullet \eta_{el}} + \frac{\dot{Q}_{Bo}}{\eta_{Bo}} \right) \bullet \Delta\vartheta \tag{30}$$

Where $T_{lettuce}$ is the total processing time of lettuce, $\Delta\vartheta$ are the time steps, which is assumed to be one hour. Then, knowing the quantity of lettuce harvested, m_p, the specific primary energy consumption, which is the amount of energy required to yield 1 *kg* of product is:

$$e_{lettuce} = \frac{E_{primary}}{m_{p\,lettuce}} \tag{31}$$

Since the energy cost is related to the source employed, Eq. (31) can be referred also to specific electricity and gas consumption:

$$e_{el} = \frac{E_{el}}{m_{p\,lettuce}}; e_{gas} = \frac{E_{gas}}{m_{p\,lettuce}} \tag{32}$$

Consequently, the specific cost for energy, namely *SCE*, per kilogram of lettuce, is evaluated knowing the specific energy consumption and the specific cost for energy (both electric c_{el} and natural gas c_{gas}):

$$SCE_{lettuce} = \sum_{i=1}^{T_{lettuce}} \left(e_{el} \bullet c_{el} + e_{gas} \bullet c_{gas}\right) \tag{33}$$

It is worth noting that this cost accounts only for energy consumption in the growing chamber. All the other zones constituting the vertical farm, whit the relative energy demand, the costs for the workforce, maintenance, machinery and all the other items to run a *VF* are outside of the purpose of this study. Moreover, implementing the same methodology for a *VF* in which more than one product is grown, the allocation of *SCE* for each product can be carried out. Finally, the same methodology could be applied also for other process inside the *VF*, accounting for the amount of product processed and the energy required for those processes as done in [32].

2.6. Resolution algorithm

The resolution algorithm, which integrates all the previously mentioned sub-models, is developed and implemented in Matlab [33] environment, with the aid of Refprop 9.1 [30] for thermodynamic and transport properties evaluation. The system is solved on a hourly basis, with the external conditions (dependent on the specific climate) being the inputs, including dry bulb temperature, relative humidity and irradiance, as well as the dimensions of the *VF*. For each operating hour, the electrical power required by the *LED* is calculated using Eqs. (1–2). The plant evapotranspiration model, described by Eqs. (3–10), is then solved to determine the internal temperature of the growth chamber, as well as the latent and sensible heat associated with the plants. Subsequently, Eqs. (11–15) are employed to estimate the heat transfer through the building envelope. Then, all the thermal loads, both sensible and latent are evaluated with Eqs. (16–18), thus the required power and gas consumption for the air conditioning system is determined to counterbalance these loads, with Eqs. (19–25). Using the electrical efficiency of the national grid of the city considered, and a fixed boiler efficiency, equal to 0.9, the primary energy consumption is evaluated. Finally, the total and specific costs are determined by considering the calculated yield and the specific cost of electricity and natural gas consumption, Eqs. (30–33).

3. Case study description and sensitivity analysis

3.1. Vertical farm layout

The developed model is employed to assess energy consumption of a *VF* growth chamber, focusing on green lettuce cultivation. The growth

Table 2
Geometrical and structural features for the employed vertical farm.

Parameter	Value	Parameter	Value	Parameter	Value
Cell length L [m]	48	Cell height H [m]	7.2	Cell width W [m]	6.5
Climate zone	Naples, Stockholm, Riyadh	Radiation converted in mol $\eta_{leafPAR}$ [$\mu mol \bullet J^{-1}$]	2.3	Wall thickness Δx [m]	0.1
Absorption coefficient α [-]	0.25	Growth cycle duration [day]	29	Wall thermal conductivity k_{wall} [$W \bullet m^{-1} \bullet K^{-1}$]	0.023
Photoperiod duration [h]	16	Specific heat of the wall insulating material c_{wall} [$kJ \bullet kg^{-1} \bullet K^{-1}$]	1.5	Density of the wall insulating material ρ_{wall} [$kg \bullet m^{-3}$]	122
Number of racks in the growth cell [-]	5	Number of cycles during theYear [-]	12	Leaf reflection coefficient R [-]	0.05
Reference yield Y_{ref} [$kg \bullet m^{-2}$]	6.25	$PPFD_{target}$ [$\mu mol \bullet m^{-2} s^{-1}$]	250	Internal convective heat transfer coefficient h_{int} [$W \bullet m^{-2} \bullet K^{-1}$]	7.7
Leaf area index LAI [-]	2.1	Vapor concentration deficit VCD [$kg \bullet m^{-3}$]	$5 \bullet 10^{-3}$	CAC[-]	0.95
Optimal leaf surface temperature T_{opt} [$^{\circ}C$]	24	Maximum leaf surface temperature T_{max}[$^{\circ}C$]	29	Target relative humidity in the cell ϕ_{cell}[%]	75

chamber layout remains consistent across all investigated climates, as does the choice of insulation material and the thickness of the external wall. Fig. 4 presents a schematic layout of the growth chamber, including its dimensions, while Table 2 provides the key geometric and structural characteristics.

3.2. Climate conditions

*VF*s are a very promising solution in hot and arid climate, where water availability is poor, as well as in large cities where on-site vegetable production can reduce transportation costs and environmental impact, ensuring the food security and the high demand satisfaction. However, these systems have a significant energy consumption, with the air conditioning system accounting for a considerable share of the total energy usage. Therefore, it is important to analyze the impact of external climate conditions, as they influence the cooling and heating requirements. For this reason, in this study, three distinct climates are considered: Naples, Stockholm, and Riyadh, which represent a Mediterranean climate, a very cold one, and a hot and arid one, respectively. By examining these different climates, valuable insights can be gained regarding their specific effects on cooling and heating demands within *VF* systems. In detail, for each climate zone, the annual climate conditions in terms of external ambient temperature, relative humidity, solar radiation and wind velocity are taken from PVGIS database [34].

In Fig. 5 are reported the annual relative humidity and temperature profiles for the three cities.

3.3. Sensitivity analysis

Since the main objective of the work is to evaluate the total and the specific energy consumption and costs for a *VF*, a preliminary sensitivity analysis is carried out in order to investigate the effect of different independent variables on the objective parameters. Particularly, the variables considered are reported in Table 3 altogether with their variation range, selected according to the range found in the scientific literature. Particularly, T_{leaf} (leaf surface temperature during the illumination periods) varies between 22 and 28 °C [12,24,25]; the *PPFD* is included between 250 $\mu mol \bullet m^{-2} \bullet s^{-1}$ and 700 $\mu mol \bullet m^{-2} \bullet s^{-1}$, as reported in [17,26,27] and η_{LED} (efficiency of the lighting system) varies between 0.35 and 0.6, according to the literature [15,17] and a market analysis.

The first two parameters, T_{leaf} and *PPFD* are directly linked to plant growth and yield, as demonstrated by equations (26–29). However, they also have an impact on energy consumption. For these reasons a sensitivity analysis is carried out by means a brute-force search, investigating all the possible solutions made up by combining the parameters reported in Table 3. The results of the sensitivity analysis are presented using the Spearman coefficient, which ranges from −1 (indicating a decrease of the objective function with the independent variables) to 1. Fig. 6 (a) illustrates the impact of the independent variables on total primary energy consumption, total primary energy cost, and productivity. It is evident that an increase in η_{LED} has no effect on productivity but provides significant advantages in terms of reduced yearly energy consumption and energy costs, with a Spearman coefficient of approximately −0.71. Conversely, an increase in *PPFD*, despite leading to higher productivity, results in a substantial rise in both primary energy consumption and costs, with a Spearman coefficient of 0.67. The increase in leaf surface temperature, on one hand, leads to a significant decrease in productivity after reaching an optimum temperature of 24 °C. On the other hand, it has negligible effects on energy consumption and costs, as it only causes a minor variation in the cell temperature and, consequently, the *HVAC* system's energy consumption.

In Fig. 6 (b) the results of the sensitivity analysis in terms of specific values are shown. Particularly, the *LED* efficiency has the same effect as on the total parameters. The increase of the *PPFD*, causing both a rise on productivity and consumption, also causes a slight rise in the primary

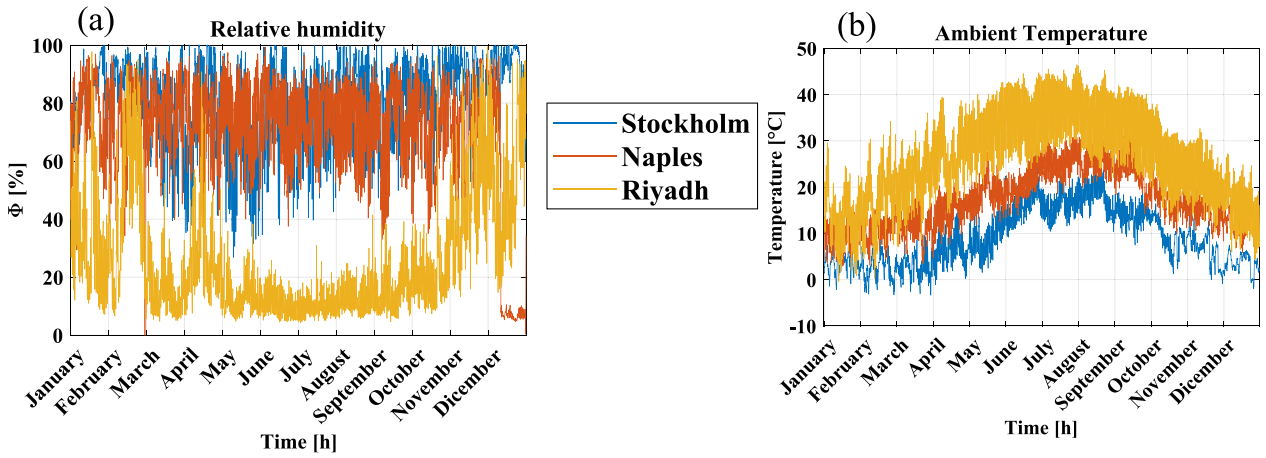

Fig. 5. (a) Annual relative humidity profile and (b) annual temperature profile for the three considered climate zones of Stockholm, Naples and Riyadh.

Table 3
Sensitivity analysis parameters and their variation range.

Parameter	Value
T_{leaf} [°C]	22–23-24–25-26–27-28
$PPFD$ [$\mu mol \bullet m^{-2} \bullet s^{-1}$]	250–325–400-475–550-625–700
η_{LED} [-]	0.35–0.4–0.5–0.55–0.6

energy specific consumption and *SCE*, due to a higher increase of consumption with respect to productivity. Finally, since the enhancement of the surface temperature strongly decreases the productivity, but is not effective on the total consumption, the specific energy consumption and the *SCE* dramatically grow, with a Spearman of almost 0.6.

4. Energy analysis

4.1. Effect of operating parameters on primary energy consumption

In this section the effect of the operating parameters on total primary energy demand and on primary energy distribution among the different component of the system is presented, considering the national electric efficiencies reported in [35,36]. Particularly, for Riyadh, Naples and Stockholm, the national electrical system efficiencies are respectively 0.4, 0.53 and 0.72. For each city the effect of *PPFD*, leaf surface temperature and *LED* efficiency is shown, from Figs. 7-10. Particularly, both, the total energy demand, Fig. 7 (a) to Fig. 10 (a), and the percentage distribution of energy demand among the different energy carrier (*LED*, chiller, boiler and circulating fan), Fig. 7 (b) to Fig. 10 (b) are displayed.

Fig. 7 illustrates the effect of *PPFD* for a leaf surface temperature of 24 °C and a *LED* efficiency of 0.6. It is evident, from Fig. 7 (a), that increasing the *PPFD* from 250 to 700 $\mu mol \bullet m^{-2} \bullet s^{-1}$ the total energy consumption dramatically rises. Specifically, it increases by 155 % in Riyadh, from 3.98 to 10.1 $GWh \bullet year^{-1}$, by 139 % in Naples, from 3.06 to 7.32 $GWh \bullet year^{-1}$ and by 122 % in Stockholm, from 2.4 to 5.4 $GWh \bullet year^{-1}$. It is also noticeable that, for a fixed *PPFD* the energy consumption is higher in Riyadh than in the other two cities. In comparison to Naples, it is between 30 % and 38 % larger, while in relation to Stockholm, it is between 62 % and 86 % higher. However, it should be specified that these discrepancies are primarily due to differences in the efficiency of the national electrical grids. To account for this, the results are also presented considering the same electrical grid efficiency, equal to 0.5 (Fig. 8). In this case, as shown in Fig. 8 (a), the system in Riyadh remains the most energy-consuming, but the greater discrepancy is approximately 0.7 $GWh \bullet year^{-1}$. Warm climates experience both a higher cooling demand and lower seasonal energy efficiency ratio (*SEER*), as defined in [31], contributing to augmented total primary energy consumption of them in Riyadh, followed by Naples and Stockholm. Fig. 7 (b) and Fig. 8 (b) confirm that in warmer climate the relative percentage of energy required by the *HVAC* on the total demand is heavier with respect to colder climate. Moreover, the increase in the *PPFD* leads to a rise in the ratio between energy required by the lighting system and the total.

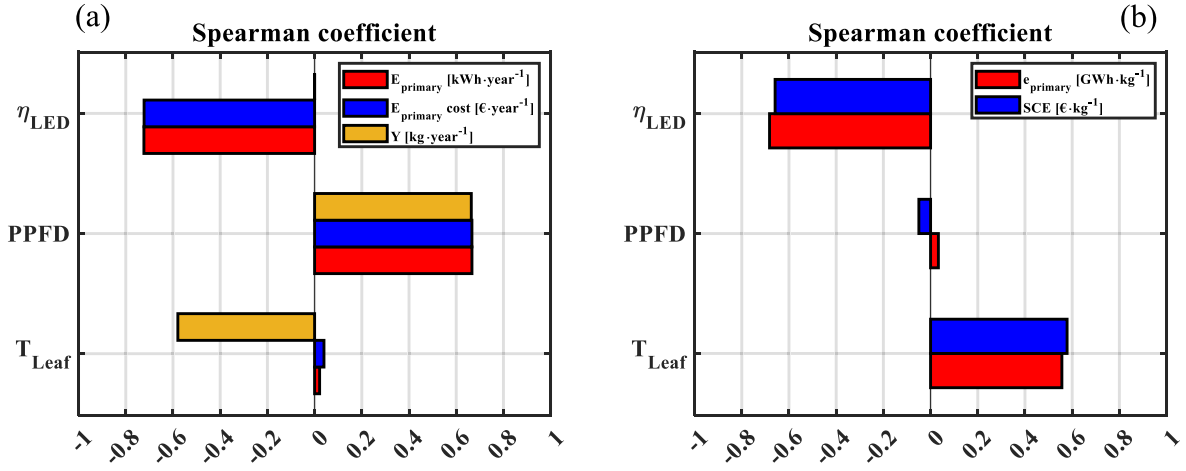

Fig. 6. Sensitivity analysis results. Effect of LED efficiency, PPFD and leaf surface temperature on: (a) total primary energy consumption, total primary energy cost (TCE) and annual productivity; (b) specific energy consumption and on the SCE.

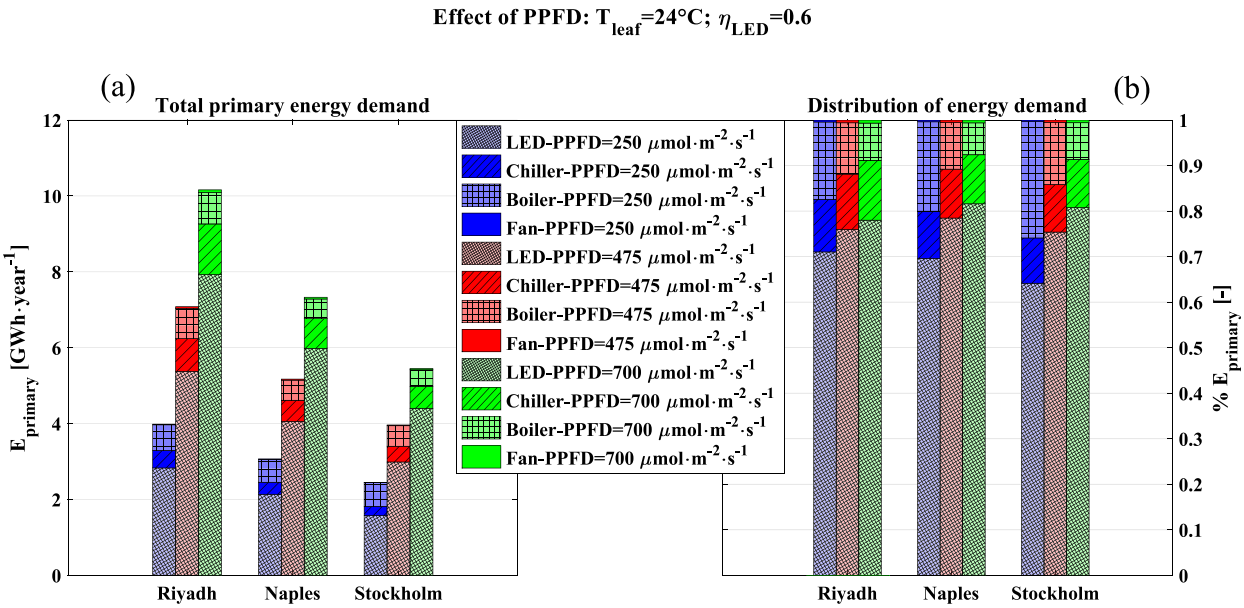

Fig. 7. Effect of the PPFD level on the total energy demand (a) dimensional plot and (b) percentage plot for a leaf surface temperature of 24 °C and a LED efficiency of 0.6 for the three considered climate zones of Riyadh, Naples and Stockholm.

In Fig. 9 the effect of η_{LED} is shown for a leaf surface temperature of 24 °C and a *PPFD* of 250 $\mu mol \bullet m^{-2} \bullet s^{-1}$. From Fig. 9 (a), it is evident that lower *LED* efficiency results in a significant increase in energy consumption. This efficiency not only directly influences the energy demand of the *LED* but also indirectly affects the *HVAC* load due to increased heat losses and consequently a higher sensible heat released in the internal environment, that has to be counterbalanced by the cooling system, leading to higher chiller energy consumption. Specifically, for the climate of Riyadh, increasing η_{LED} from 0.35 to 0.6 leads to a decrease in *LED* energy consumption from 6.3 to 2.8 $GWh \bullet year^{-1}$. Within the same range of η_{LED} primary energy consumption related to the chiller decreases from 0.98 to 0.46 $GWh \bullet year^{-1}$. When comparing the different cities, it is important to note that the discrepancies in consumption are, in this case as well, influenced by the diverse efficiencies of the electrical grids.

Fig. 9 (b) highlights that the increase of the *LED* efficiency brings to a reduced percentage of energy required by the lighting system and by the chiller (since decreases the cooling demand), consequently, despite it remains unchanged the absolute energy demand for re-heating purposes, it increases the share of energy required by the boiler.

In Fig. 10 it is reported the effect of leaf surface temperature. As shown in Fig. 10 (a), it does not affect at all the *LED* consumption, but given its influence on the cell temperature (described in Eq. (10)) it impacts on the cooling demand and the chiller energy consumption. In

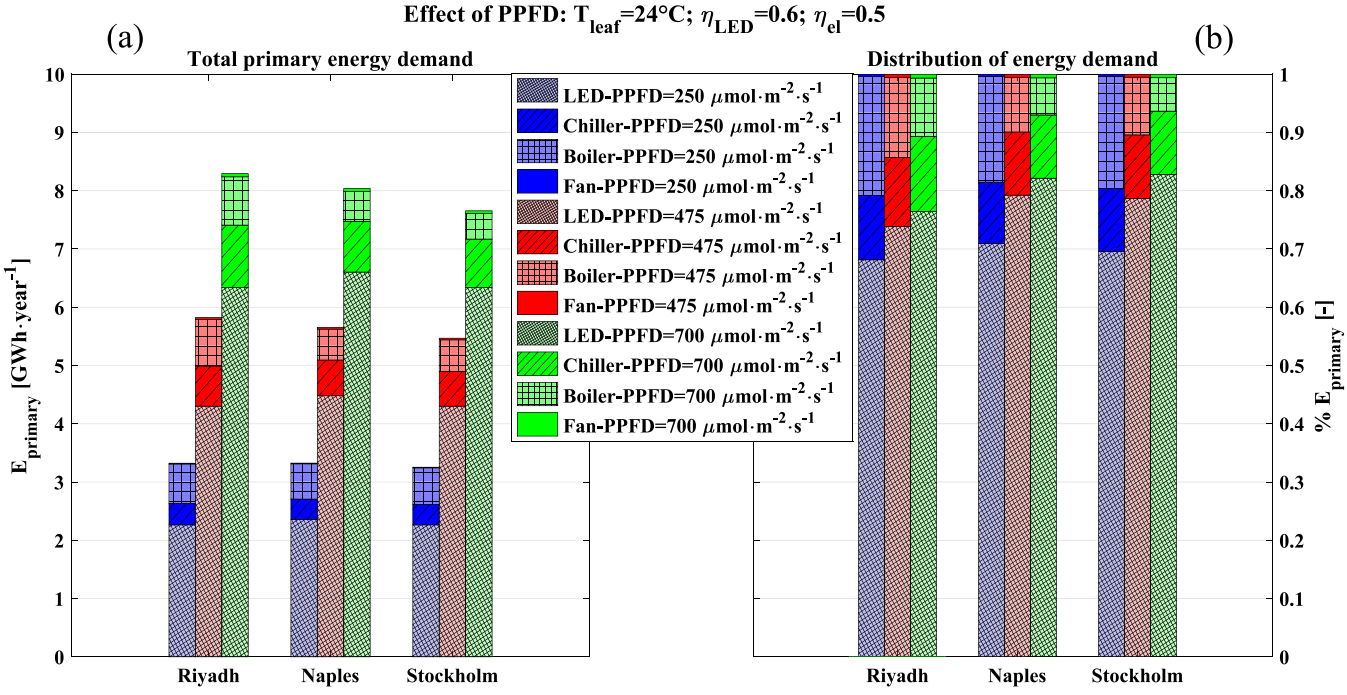

Fig. 8. Effect of the PPFD level on the total energy demand (a) dimensional plot and (b) percentage plot for a leaf surface temperature of 24 °C, LED efficiency of 0.5 and efficiency of the electrical grid of 0.5 for the three considered climate zones of Riyadh, Naples and Stockholm.

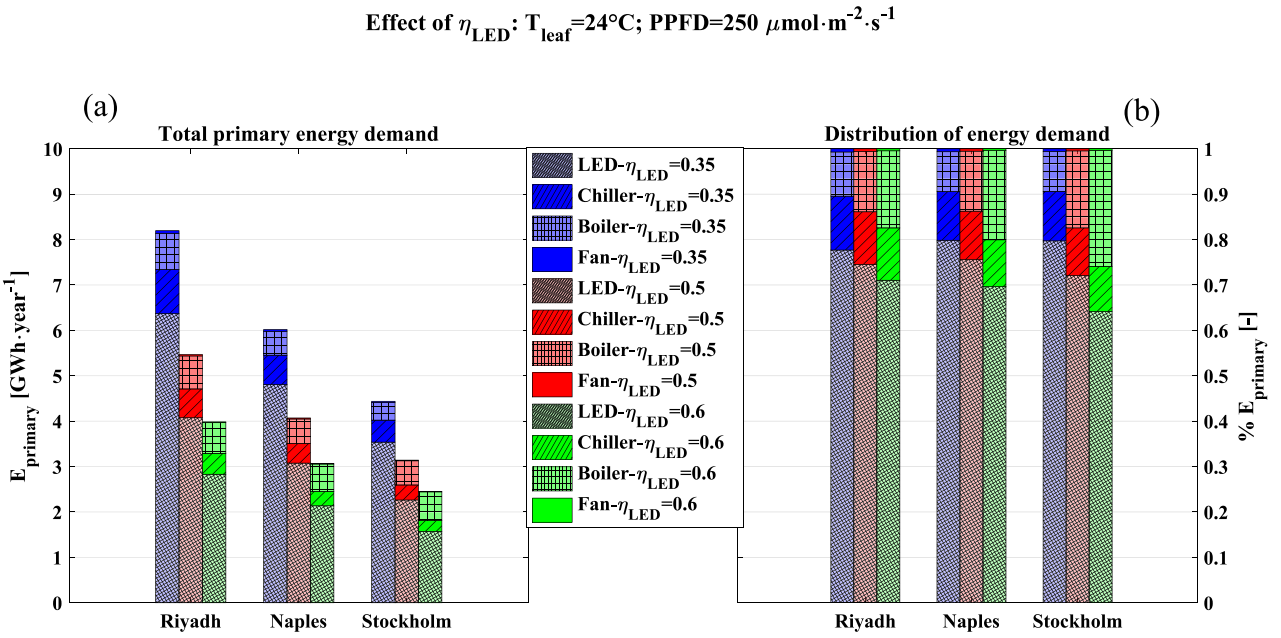

Fig. 9. Effect of the LED efficiency on the total energy demand (a) dimensional plot and (b) percentage plot for a leaf surface temperature of 24 °C and a PPFD value of 250 $\mu mol \bullet m^{-2} \bullet s^{-1}$ for the three considered climate zones of Riyadh, Naples and Stockholm.

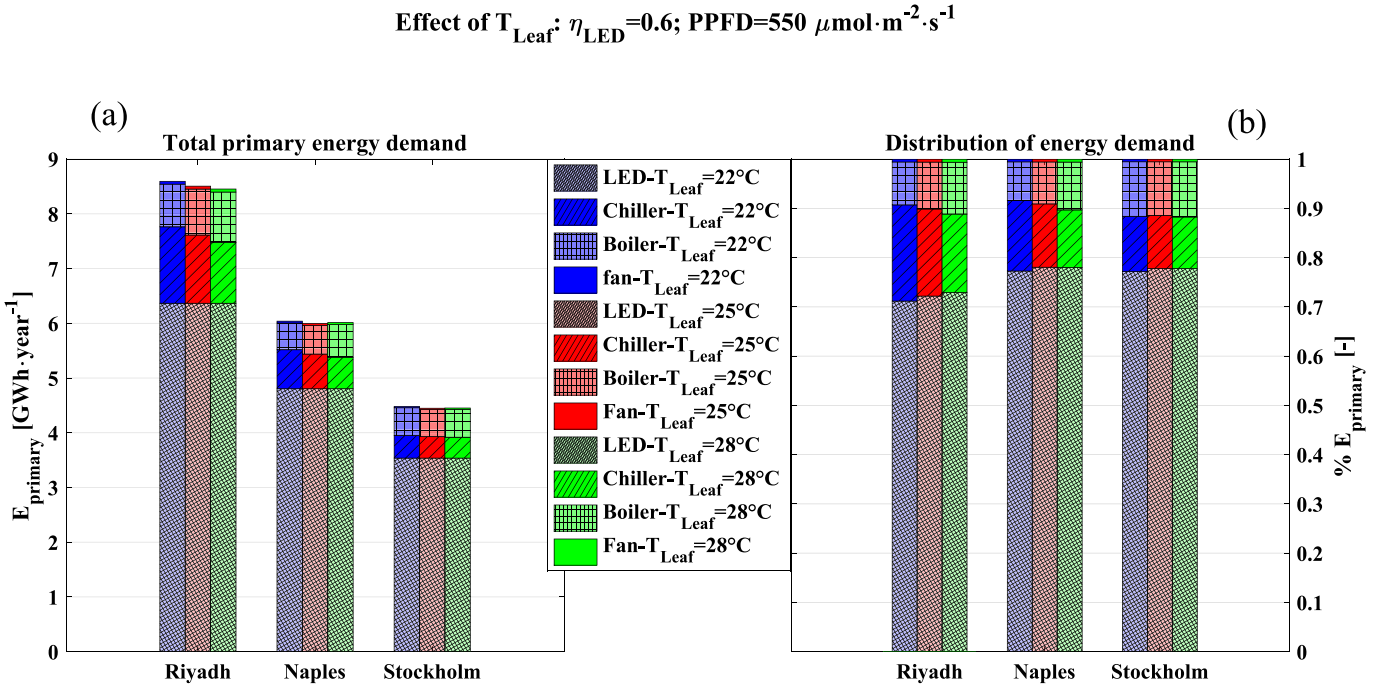

Fig. 10. Effect of the leaf surface temperature on the total energy demand (a) dimensional plot and (b) percentage plot for a LED efficiency of 0.6 and a PPFD level of 550 $\mu mol \bullet m^{-2} \bullet s^{-1}$ for the three considered climate zones of Riyadh, Naples and Stockholm.

fact, for a lower leaf temperature an inferior temperature in the cell has to be guaranteed, and thus a higher cooling demand is required to the chiller. Similarly to previous findings, the discrepancies among the three climates are attributed to differences in η_{el} and SEER decrease in warmer climates. From Fig. 10 (b) it is also evident that the leaf surface temperature has a negligible effect also on distribution of the energy demand among different carriers.

As specified in the section 2.3, related to HVAC modelling, the refrigerant in the chiller is R134a, being traditionally one of the most employed due to its thermophysical properties. However, for comparison purposes, some simulations, not reported in the paper, are carried out also with its low global warming impact replacement, namely R1234ze(E), highlighting that the chiller consumption increases between the 3.9 % and the 25 % with the HFO refrigerant.

4.2. Effect of investigated parameters on the yield

In Fig. 11 the leaf surface temperature and PPFD effect on annual yield is shown. In detail, it is evident that for a given *PPFD* the maximum yield is achieved for a T_{leaf} of 24 °C. Particularly, at this leaf surface temperature and with a *PPFD* of 700 $\mu mol \bullet m^{-2} \bullet s^{-1}$ a yield of 270 $Ton \bullet year^{-1}$ is reached. For T_{leaf} higher than 26 °C the annual yield dramatically decreases, dropping more than the 70 %.

Fig. 12 shows the relation between the yearly yield per m^2 and primary energy consumption per m^2, for the climate zone of Stockholm and for a fixed *LED* efficiency and various leaf surface temperature and *PPFD* shown in Table 3. As previously underlined, the higher effect on yield is attributable to leaf surface temperature, with differences above 300 % augmenting T_{leaf} from 22 °C to 28 °C (increasing firstly, until the maximum reached at 24 °C and then dramatically decreasing). The energy consumption, instead, rises mostly with *PPFD*, almost with a linear trend, increasing from 1.78 $MWh \bullet m^{-2} \bullet year^{-1}$ to approximately 4.10 $MWh \bullet m^{-2} \bullet year^{-1}$.

4.3. Effect of investigated parameters on specific energy consumption

Fig. 13 displays the leaf surface temperature and *LED* efficiency effect on specific energy consumption $e_{primary}$ for the city of Naples. This term represents the ratio between total energy demand, $E_{primary}$, and total yield, namely the energy consumption per kg per year, as described by Eq. (34):

$$e_{primary} = \frac{E_{primary}}{Yield} \tag{34}$$

It can be seen that $e_{primary}$ decreases when T_{leaf} increases from 22 °C to 24 °C and then it rises sharply when T_{leaf} augments from 24 °C to 26 °C. With a further increase of leaf surface temperature $e_{primary}$ rises dramatically. This is because despite the influence of T_{leaf} on energy consumption is negligible, it strongly affects the yield, which decreases remarkably for temperatures higher than 26 °C. A remarkable reduction in $e_{primary}$ is attributable also to a *LED* efficiency increase, due to a drop of lighting system and *HVAC* consumption, while the yield results unaffected. The effect of *PPFD* is, instead, negligible, since its rise causes also a slightly increase on $e_{primary}$, because the augment in the energy consumption is counterbalanced by yield increase.

4.4. Effect of operating parameters on energy cost

In this section the *SCE* is presented for each climate with respect to the operating parameters investigated and considering different scenarios of energy cost. Particularly, the electric energy cost varies between 0.05 and 0.3 $€ \bullet kWh^{-1}$ while the natural gas price ranges between 0.75 and 2 $€ \bullet Sm^{-3}$. Such a wide range of cost for energy is chosen to take into account the uncertainty of the market, depending on multiple factors, which make it impossible to crystallize the energy cost, and thus to explore a large number of cases.

Fig. 14 shows the specific cost map for the investigated system in the city of Naples for a specific cost of electricity of 0.1 $€ \bullet kWh^{-1}$ and a specific cost of natural gas of 1 $€ \bullet Sm^{-3}$. Notably, the leaf temperature has the highest effect on *SCE*, given its significant contribution to productivity, while it has a less pronounced impact on total consumption, as shown above. The minimum *SCE* is achieved when T_{leaf} is set to 24 °C. As previously mentioned, *PPFD* has a slightly negative effect on specific energy consumption. Finally, increasing *LED* efficiency provides substantial benefits to the system's efficiency.

In Fig. 15 the relation between yield per m^2 and the primary energy cost per m^2 is depicted, for a fixed *LED* efficiency (equal to 0.6), a specific electricity cost of 0.1 $€ \bullet kWh^{-1}$ and a natural gas cost of 1 $€ \bullet Sm^{-1}$, and various leaf surface temperature and *PPFD* for the climate zone of Riyadh. The trend of yield is the same shown in Fig. 12, as well as the primary energy cost, having the same trend of the primary energy consumption described in the aforementioned figure. Consequently, the leaf surface temperature and the *PPFD* intensity have to be chosen in order to maximize the productivity reducing the primary energy consumption and the related cost per m^2.

To have a comprehensive evaluation of vegetables production in a *VF*, but also in general to assess the production of any kind of product, it is necessary to consider the effects that operating parameters have both on yield and energy demands. In some cases, these impacts can be contrasting and so their mutual influence needs to be considered simultaneously. The approach proposed in this work, based on the Specific Cost for Energy, but in general any approach based on the energy cost for unit of product, can achieve this purpose. As an example, the following Fig. 16 (a) shows the *SCE* of lettuce for different value of the *LED* efficiency and *PPFD* in a *VF* located in Naples. For the leaf surface temperature, it is assumed 24 °C because, as reported before, it minimizes specific primary energy consumption and *SCE*. In all the combinations considered, lighting expenditure has the greatest influence on *SCE*, more than 68 % (Fig. 16 (b)). It can be noted that the *SCE* drastically reduces increasing the *LED* system efficiency, with *PPFD* = 700 $\mu mol \bullet m^{-2} \bullet s^{-1}$, decreasing by three times. More in detail all the energy costs shares composing the *SCE* drop. In percentage terms (Fig. 16 (b)), when the minimum efficiency is assumed for the *LED*, the increase of *PPFD* determines a reduction in the specific expenditure for electricity required for lighting whereas, the costs to operate boiler and chiller reduce. On the contrary, with the maximum efficiency of *LED*s, as *PPFD* increases, the incidence of lighting expenditure on the unitary cost rises while the contribution due to natural gas decreases significantly. When η_{LED} is considered equal to 0.45 the greatest contribution to the unitary cost due to the power supply to the *LED*s occurs for *PPFD* = 475

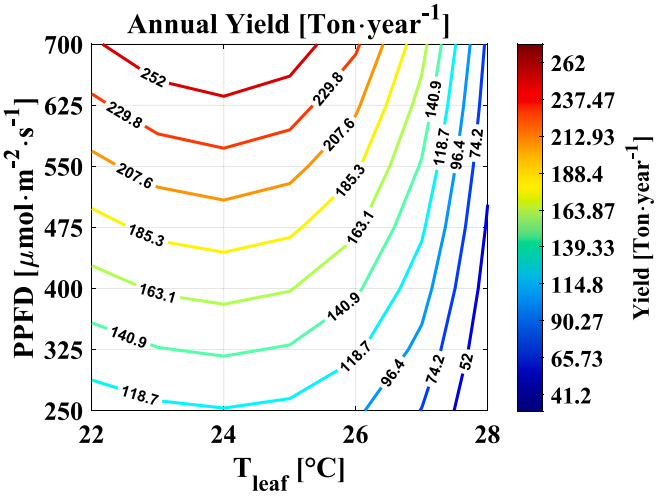

Fig. 11. Effect of leaf surface temperature and PPFD levels on the annual yield.

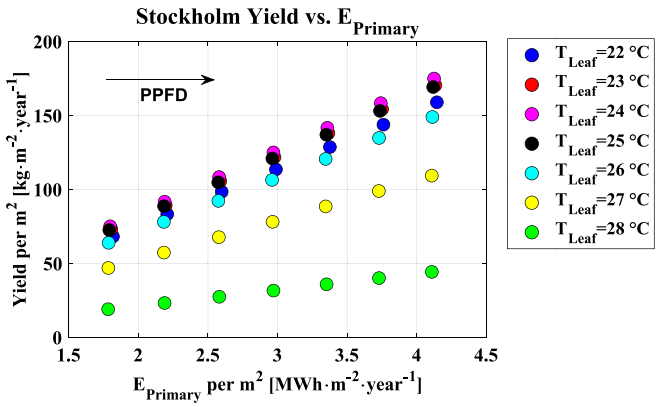

Fig. 12. Yield per m^2 with respect to primary energy consumption per m^2s for a fixed LED efficiency of 0.6 for the climate zone of Stockholm.

$\mu mol \bullet m^{-2} \bullet s^{-1}$, correspondingly there is the minimum contribution of natural gas.

From the comments reported above, it can be deduced that the modelling approach proposed in this work can help to identify what are the most energy intensive aspects of the production affecting the *SCE* and therefore those to pay attention to. In particular, it is highlighted that strong benefits can be obtained by intervening on the energy demands of the *LED*s or more generally by limiting the demands for electricity from the network.

It is equally clear from the brief considerations presented before that the proposed analysis methodology can be replicated in other production cases and incorporate further and more detailed models and information.

5. Conclusions

In this manuscript, an assessment of the energy consumption and cost related to the energy demands of a vertical farm's growth chamber, specifically for lettuce production, has been conducted. The analysis considers different climate regions, lighting system intensity and efficiency, leaf surface temperature, and economic scenarios. A dynamic simulation model of the production system (vertical farm + air-conditioning equipment) and a novel methodology to evaluate the specific cost for energy (*SCE*) are proposed. The main findings are as follows:

- The system energy consumption is significantly dependent on climate conditions. As a matter of fact, for a PPFD of 500 $\mu mol \bullet m^{-2} \bullet s^{-1}$, a leaf surface temperature of 24 °C and a LED efficiency of 0.5 the energy consumption is 38 % and 86 % higher in Riyadh (10.1 $GWh \bullet year^{-1}$) compared to Naples and Stockholm, respectively.
- The lighting system accounts for 65 % to 85 % of the primary energy consumption, followed by cooling and heating demands in the HVAC system (15 % to 20 % and 10 % to 15 % respectively), while the circulating fan requires only a minimal share of energy (lower than 1 %).
- The PPFD increase, from 250 to 700 $\mu mol \bullet m^{-2} \bullet s^{-1}$, leads to a rise in total energy consumption of 122 % in Stockholm, 139 % in Naples and 155 % in Riyadh. Simultaneously, it also causes a yield augment. Also the lighting system efficiency increase, from 0.35 to 0.6, has a great beneficial effect on both, total and specific energy consumption. The leaf surface temperature variation leads to a small increase of cooling demand for lower temperatures, thus slightly higher chiller consumption. Regarding the specific consumption, a minimum is found for a leaf temperature of 24 °C, where the maximum productivity is achieved (270 $Ton \bullet year^{-1}$).
- The economic analysis is carried out considering an electricity and natural gas cost ranging between, respectively, 0.05 and 0.3 $€ \bullet kWh^{-1}$ and 0.75 and 2 $€ \bullet Sm^{-3}$. It has been seen that the higher influence on SCE depends on electricity cost, since most of the energy request is in terms of electric energy, while only a limited percentage (between 10 and 15 %) is satisfied by natural gas. The SCE decreases rising the lighting system efficiency and ensuring a leaf surface temperature equal to 24 °C. The minimum specific cost associated to energy consumption in the growth chamber in the analyzed configurations is 0.85 $€ \bullet kg^{-1}$ in Stockholm, 1.35 $€ \bullet kg^{-1}$ in Naples and 1.75 $€ \bullet kg^{-1}$ in Riyadh.

It is worth nothing that these results only pertain to the energy consumption and costs allocation related to the growth chamber of the vertical farm and for a specific product. Further studies should consider

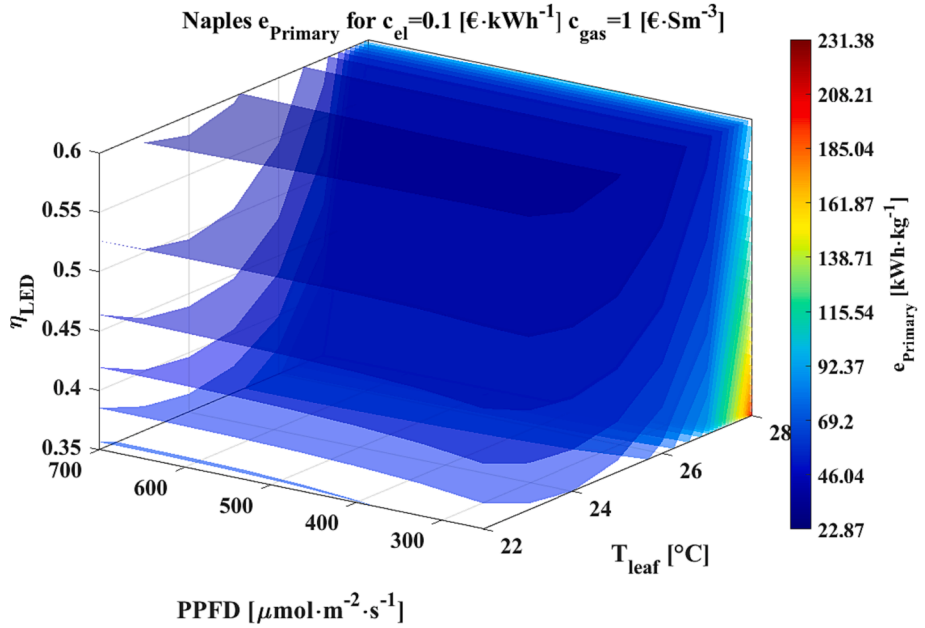

Fig. 13. Effect of the leaf surface temperature and LED efficiency on the specific energy consumption for the city of Naples.

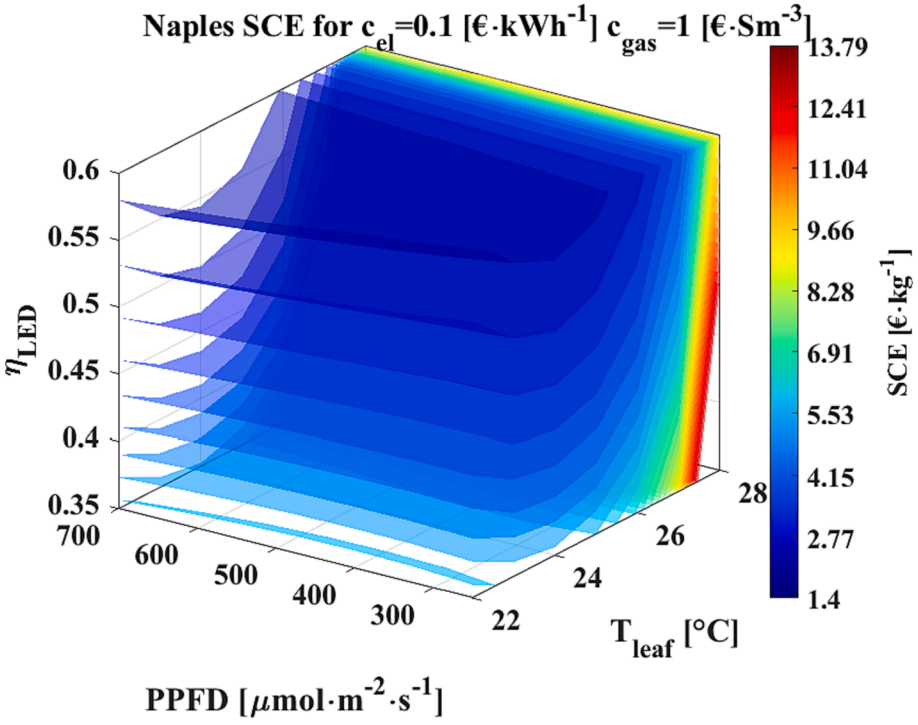

Fig. 14. Effect of the leaf surface temperature and LED efficiency on the rate of cost for energy for the city of Naples for a specific electricity cost of 0.1 € • kWh^{-1} and a specific natural gas cost of 1 € • Sm^{-3}.

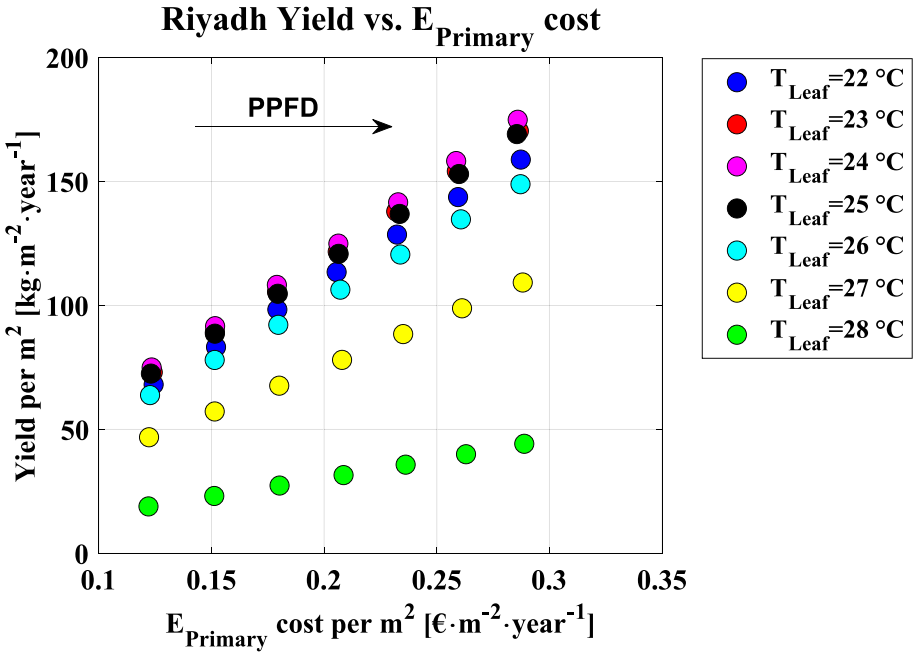

Fig. 15. Yield per m^2 with respect to primary energy cost per m^2 for a fixed LED efficiency of 0.6, for a specific electricity cost of 0.1 € • kWh^{-1} and a specific natural gas cost of 1 € • Sm^{-3} for the climate zone of Riyadh.

all other processes within the vertical farm, both pre- and post-crop growth, to quantify the total energy consumption and total specific cost of the harvested product. Additionally, a comprehensive assessment of vertical farm profitability compared to traditional systems requires an analysis of the entire supply chain, including the cold chain, transportation costs, product selling price and investment costs to build a *VF*.

CRediT authorship contribution statement

A. Arcasi: Investigation, Data curation, Writing – original draft. **A. W. Mauro:** Conceptualization, Methodology, Resources, Supervision. **G. Napoli:** Investigation, Data curation, Writing – original draft. **F. Tariello:** Investigation, Supervision, Writing – review & editing. **G.P. Vanoli:** Resources, Supervision.

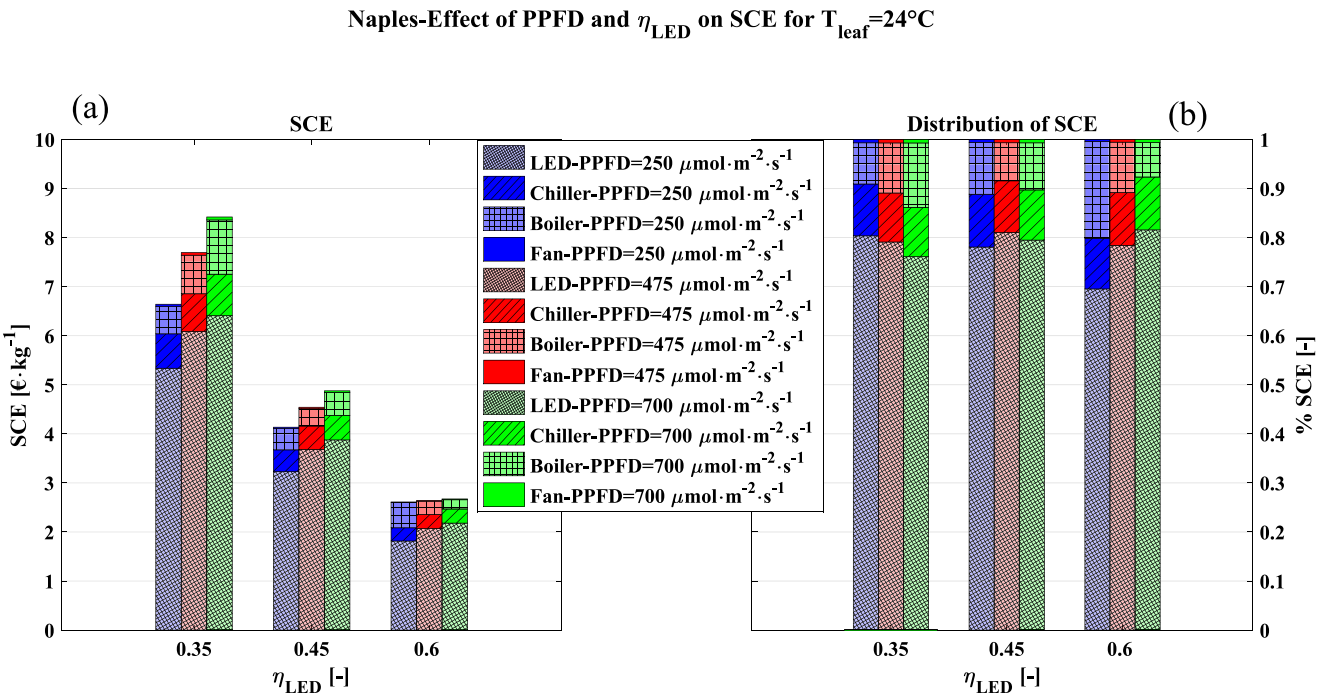

Fig. 16. Effect of the PPFD and LED efficiency on the SCE (a) dimensional plot and (b) percentage plot for a leaf surface temperature of 24 °C for the three considered climate zones of Naples, for a specific electricity cost of 0.1€ • kWh^{-1} and a specific natural gas cost of 1€ • Sm^{-3}.

Declaration of Competing Interest

The authors declare that they have no known competing financial interests or personal relationships that could have appeared to influence the work reported in this paper.

Data availability

No data was used for the research described in the article.

Acknowledgements

The project: "National research centre for agricultural technologies (Agritech)" – E63C22000920005 – "Piano Nazionale di Ripresa e Resilienza" funded by "Ministero dell'Università e della Ricerca" through funds NextGenerationEU is gratefully acknowledged

References

[1] Fao. The state of the world's land and water resources for food and agriculture (SOLAW) – Managing systems at risk. Food and Agriculture, Organization of the United Nations, Rome and Earthscan, London (2011).
[2] UNESCO, The United Nations world water development report. https://unesdoc.unesco.org/ark:/48223/pf0000225741_eng, 2014 (accessed on 14 July 2023).
[3] Eurostat Data Browser. https://ec.europa.eu/eurostat/databrowser/view/NRG_BAL_S_custom_624870/default/table?lang=en (accessed on 14 July 2023).
[4] European Commission, The World Energy Outlook to 2050 report. https://ec.europa.eu/commission/presscorner/detail/en/MEMO_07_2 (accessed on 14 July 2023).
[5] The World Bank Data. https://data.worldbank.org/indicator/AG.LND.ARBL.HA.PC?end=2020&locations=EU&start=1961&view=chart (accessed on 16 July 2023).
[6] United Nations, Department of Economic and Social Affairs, Population Division, World Population Prospects: The 2017 Revision, Key Findings and Advance Tables. Working Paper No. ESA/P/WP/248 (2017).
[7] United Nations. World urbanization prospects: the 2014 revision, highlights. Department of Economic and Social Affairs (2014). https://doi.org/10.4054/DemRes.2005.12.9.
[8] Food and Agriculture Organization of the United Nations, FAOSTAT. https://www.fao.org/faostat/en/#data/RP (accessed on 16 July 2023).
[9] United Nations. https://unric.org/it/obiettivo-2-porre-fine-alla-fame-raggiungere-la-sicurezza-alimentare-migliorare-la-nutrizione-e-promuovere-unagricoltura-sostenibile/ (accessed on 17 July 2023).
[10] T. Kozai, Resource use efficiency of closed plant production system with artificial light: Concept, estimation and application to plant factory, Proceedings of the Japan Academy Ser. B Physical and Biological Sciences 89(10), (2013) 447-461. 10.2183/pjab.89.447.
[11] K. Al-Kodmany, The Vertical Farm: A Review of Developments and Implications for the Vertical City, Buildings 8 (2) (2018) 24, https://doi.org/10.3390/buildings8020024.
[12] L. Graamans, E. Baeza, A. van den Dobbelsteen, I. Tsafaras, C. Stanghellini, Plant factories versus greenhouses: Comparison of resource use efficiency, Agr. Syst. 160 (2018) 31–43, https://doi.org/10.1016/j.agsy.2017.11.003.
[13] K. Benke, B. Tompkins, Future food-production systems: vertical farming and controlled-environment agriculture, Sustainability: Science, Pratice and Policy 13 (1) (2017) 13–26, https://doi.org/10.1080/15487733.2017.1394054.
[14] M. Gentry, Local heat, local food: Integrating vertical hydroponic farming with district heating in Sweden, Energy 174 (2019) 191–197, https://doi.org/10.1016/j.energy.2019.02.119.
[15] K. Harbrick, L.D. Albright, Comparison of energy consumption: greenhouses and plant factories, Proc. VIII Int, Symp. on Light in Horticulture (2016), https://doi.org/10.17660/ActaHortic.2016.1134.38.
[16] J.-E. Park, H. Kim, J. Kim, S.-J. Choi, J. Ham, C.W. Nho, G. Yoo, A comparative study of ginseng berry production in a vertical farm and an open field, Ind. Crop. Prod. 140 (2019), 111612, https://doi.org/10.1016/j.indcrop.2019.111612.
[17] D.D. Avgoustaki, G. Xydis, Indoor Vertical Farming in the Urban Nexus Context: Business Growth and Resource Savings, Sustainability 12 (5) (2020) 1965, https://doi.org/10.3390/su12051965.
[18] E. Molin, M. Martin, Assessing the energy and environmental performance of vertical hydroponic farming, Report C 299 (2018), https://doi.org/10.13140/RG.2.2.28444.77442.
[19] M. Martin, M. Elnour, A. Cabrero Sinol, Environmental life cycle assessment of a large-scale commercial vertical farm, Sustainable Production and Consumption 40 (2023) 182–193, https://doi.org/10.1016/j.spc.2023.06.020.
[20] L. Graamans, M. Tenpierik, A. van den Dobbelsteen, C. Stanghellini, Plant factories: Reducing energy demand at high internal heat loads through façade design, Appl. Energy 262 (2020), 114544, https://doi.org/10.1016/j.apenergy.2020.114544.
[21] L. Graamans, A. van den Dobbelsteen, E. Meinen, C. Stanghellini, Plant factories: crop transpiration and energy balance, Agr. Syst. 153 (2017) 138–147, https://doi.org/10.1016/j.agsy.2017.01.003.
[22] D.D. Avgoustaki, G. Xydis, Energy cost reduction by shifting electricity demand in indoor vertical farms with artificial lighting, Biosyst. Eng. 211 (2) (2021) 219–229, https://doi.org/10.1016/j.biosystemseng.2021.09.006.
[23] R.A. Yalcin, H. Erturk, Improving crop production in solar illuminated vertical farms using fluorescence coatings, Biosyst. Eng. 193 (2020) 25–36, https://doi.org/10.1016/j.biosystemseng.2020.02.007.
[24] T. Weidner, A. Yang, M.W. Hamm, Energy optimisation of plant factories and greenhouses for different climatic conditions, Energ. Conver. Manage. 243 (10170) (2021), 114336, https://doi.org/10.1016/j.enconman.2021.114336.
[25] L. Carotti, A. Pistillo, I. Zauli, D. Meneghello, M. Martin, G. Pennisi, G. Gianquinto, F. Orsini, Improving water use efficiency in vertical farming: Effects of growing

systems, far-red radiation and planting density on lettuce cultivation, Agric Water Manag 285 (2023), 108365, https://doi.org/10.1016/j.agwat.2023.108365.
[26] L. Carotti, L. Graamans, F. Puksic, M. Butturini, E. Meinen, E. Heuvelink, C. Stanghellini, Plant Factories Are Heating Up: Hunting for the Best Combination of Light Intensity, Air Temperature and Root-Zone Temperature in Lettuce Production, Frontiers in Plant Science 11 (2021), 592171, https://doi.org/10.3389/fpls.2020.592171.
[27] T. Jayalath, M.W. van Iersel, Canopy Size and Light Use Efficiency Explain Growth Differences between Lettuce and Mizuna in Vertical Farms, Plants 10 (4) (2021) 704, https://doi.org/10.3390/plants10040704.
[28] N. Bishara, G. Pernigotto, A. Prada, M. Baratieri, A. Gasparella, Experimental determination of the building envelope's dynamic thermal characteristics in consideration of hygrothermal modelling – Assessment of methods and sources uncertainty, Energ. Buildings 236 (2021), 110798, https://doi.org/10.1016/j.enbuild.2021.110798.
[29] H. Montazeri, B. Blocken, New generalized expressions for forced convective heat transfer coefficients at building façades and roofs, Build. Environ. 119 (2017) 153–168, https://doi.org/10.1016/j.buildenv.2017.04.012.
[30] E. W. Lemmon, M. O. Mc Linden, M. L. Huber, REFPROP NIST Database 23 (2009).
[31] Commission Regulation (EU) 2016/2281 of 30 November 2016.
[32] A. Arcasi, A.W. Mauro, G. Napoli, A.M. Pantaleo, Pantaleo, Energy cost impact analysis on the total cost of the crop production for different operating conditions. A salad production case study, 36th International Conference on Efficiency, Cost, Optimization, Simulation and Environmental Impact of Energy Systems, ECOS 2023 (2023) 2626–2636, https://doi.org/10.52202/069564-0236.
[33] MATLAB 2019a Release, Mathworks.
[34] E. Commission, Photovoltaic Geographical Information System (PVGIS), accessed on 26 June 2023, http://re.jrc.ec.europa.eu/pvgis/, 2017.
[35] ISPRA. Report 346. Efficiency and decarbonization indicator for total energy consumption and power sector (2021).
[36] Energy Central. https://energycentral.com/c/gn/look-electricity-generation-saudi-arabia-2019-so-far (accessed on 18 July 2023).